Advances in Military Technology
Vol. 21, No. 1, 2026, pp. 263-276
ISSN 1802-2308, eISSN 2533-4123
DOI 10.3849/aimt.02075

Superplastic Properties of Ultrafine-Grained AA6061 Alloy Fabricated by Cyclic Expansion-Extrusion

D. Giang Lai, M. Tien Nguyen[1], X. Truong Do[2], and I. Pemčák[3*]

[1] *Faculty of Mechanical Engineering, Le Quy Don Technical University, Ha Noi, Viet Nam*
[2] *Factory Z119, Air Defence – Air Force, Ha Noi, Viet Nam*
[3] *Department of Weapons and Ammunition, University of Defence, Brno, Czech Republic*

The manuscript was received on 5 January 2026 and was accepted after revision for publication as a case study on 22 May 2026.

Abstract:

This paper investigates the superplastic behavior of AA6061 aluminum alloy processed by cyclic expansion-extrusion, a severe plastic deformation method producing ultrafine-grained structures. Cylindrical specimens underwent up to four cyclic expansion–extrusion cycles at room temperature. The average grain size decreased from ~100 µm (annealed state) to 5–6 µm after four cycles, with nearly 75 % higher and more homogeneous microhardness. The refined microstructure fulfils conditions for superplasticity dominated by grain boundary sliding at elevated temperatures. Tensile tests showed a maximum elongation of ~330 % at 530 °C and strain rate 10^{-3} s^{-1}, with a low maximum flow stress of 9.5 MPa. The results confirm cyclic expansion–extrusion as an effective route to enhance microhardness and enable superplastic forming of lightweight AA6061 alloys.

Keywords:

AA6061 aluminum alloy, cyclic expansion-extrusion, ultrafine grains, severe plastic deformation, superplastic properties, superplastic forming

1 Introduction

Aluminum alloys are among the most widely utilized lightweight structural materials in modern engineering applications, particularly in the aerospace, automotive, marine, and defense industries. Their favorable attributes include a high strength-to-weight ratio, good corrosion resistance, and relatively easy formability compared with steels. Among these alloys, the AA6061 series, belonging to the Al-Mg-Si family, has attracted considerable attention due to its balanced combination of mechanical strength,

* *Corresponding author: Department of Weapons and Ammunition, University of Defence, Brno, Kounicova 156/65, CZ-662 10 Brno, Czech Republic. Phone: +420 973 44 36 20, E-mail: ivan.pemcak@unob.cz. ORCID 0009-0000-2224-4792.*

weldability, and corrosion resistance. These properties make AA6061 a promising candidate for components that demand both lightweight characteristics and durability under service conditions. Nevertheless, its formability under conventional processing conditions is limited. Typical tensile elongation at room temperature rarely exceeds 10–15 %, and in certain tempers, the alloy exhibits elongations of only 5–8 % [1–3]. Such limited ductility imposes constraints on the use of AA6061 in the production of thin-walled or intricately shaped parts, where extensive plastic deformation is required. Therefore, strategies for enhancing both the strength and ductility of this alloy remain of significant technological interest.

One effective approach to overcome these challenges is through the refinement of microstructures to the ultrafine-grained (UFG) regime, in which the average grain size is reduced below 10 μm. Materials with UFG microstructures often exhibit remarkable combinations of mechanical strength and plasticity [4, 5]. In particular, UFG alloys can display superplasticity – an exceptional capability to undergo very large elongations (usually above 200 %) at elevated temperatures without localized necking. This phenomenon, which is governed primarily by grain boundary sliding (GBS), occurs when a material satisfies several key conditions: fine and stable grains (generally < 10 μm), a testing temperature within 0.5–0.7 of the absolute melting point, and an optimized strain rate typically between 10^{-4} and 10^{-2} s^{-1} [6, 7]. When these criteria are fulfilled, deformation proceeds predominantly through cooperative grain boundary mechanisms rather than conventional dislocation glide, resulting in high elongation with relatively low flow stresses. Consequently, superplasticity has been exploited in SPF technologies to manufacture lightweight, complex-shaped components with reduced forming forces and enhanced design flexibility [8–10].

To generate UFG structures in bulk metallic materials, severe plastic deformation (SPD) methods have been extensively studied. These processes impose very high plastic strains without substantially altering the overall geometry of the workpiece, thereby enabling the accumulation of large strain levels necessary for grain refinement [11, 12]. Common SPD techniques include equal channel angular pressing (ECAP) [13], high pressure torsion (HPT) [14], multidirectional forging (MDF) [15], and cyclic extrusion compression (CEC) [16]. Each method has its own advantages and drawbacks. ECAP can effectively produce uniform UFG microstructures but often suffers from tool wear and dimensional limitations. HPT enables extreme grain refinement down to the nanometer scale but is constrained to small specimen sizes and requires high pressure apparatus. MDF is relatively simple in equipment but requires repeated reorientation of the specimen, which is time-consuming. CEC, on the other hand, achieves significant refinement but involves complex die designs and difficulties in controlling back pressure.

The cyclic expansion-extrusion CEE process has been proposed as a promising SPD method that combines the principles of upsetting and extrusion in a repetitive sequence. The technique involves transferring the specimen between expanded and contracted die cavities, thereby subjecting the material to alternating compressive and tensile stresses. Unlike CEC, the die geometry in CEE is relatively simple, and the material flow itself generates a back-pressure-like effect that promotes homogeneous deformation. Repeated CEE cycles gradually fragment coarse grains, induce high dislocation densities, and ultimately promote the formation of UFG microstructures through mechanisms such as continuous dynamic recrystallization. Previous studies have confirmed that CEE can refine the grain size of AA6061 from approximately 100 μm in the annealed condition to below 10 μm after several cycles, along with a marked increase in microhardness [17–19]. However, most of these investigations have focused on microstructural evolution and strengthening mechanisms, whereas the superplastic potential of AA6061 processed by CEE has received limited attention.

Superplasticity in aluminum alloys has been extensively demonstrated in systems such as AA7075, Al-Mg-Sc-Zr, and Al-Cu alloys after SPD processing [20–22]. These alloys commonly exhibit elongations exceeding 200–300 % with flow stresses below 15 MPa when tested under optimal superplastic conditions. The dominant mechanism in such cases is GBS assisted by diffusion and dynamic recovery processes, which allow grains to maintain an equiaxed morphology even at large strains. The potential to extend similar superplastic performance to AA6061 processed by CEE is highly attractive, since it would combine the alloy's inherent corrosion resistance and weldability with exceptional formability. This synergy could enable new applications in aerospace and automotive forming technologies, where lightweight components with complex geometries are increasingly demanded.

Despite the growing recognition of CEE as an effective SPD route, systematic studies on the correlation between its grain refinement effect and the superplastic behavior of AA6061 are still scarce. Most existing research has concentrated either on the simulation of deformation fields during CEE or on microhardness evaluations after processing [17, 23]. Comprehensive experimental assessments of superplasticity such as elongation to failure and flow stress at different strain rates, have yet to be fully established. Therefore, there exists a research gap in understanding whether the UFG structures produced by CEE are capable of providing the grain stability and strain rate sensitivity required for superplastic deformation.

In this paper, AA6061 specimens were processed through multiple cycles of CEE at room temperature, followed by a systematic evaluation of their microstructures and mechanical properties. The effectiveness of CEE in refining the microstructure and enhancing material strength was assessed through microstructural observations and microhardness measurements. The superplastic potential of the alloy was evaluated via deformation tests conducted under varying strain rates and temperatures. This study demonstrates that CEE not only improves the mechanical properties of AA6061 but also represents a promising processing route to unlock its superplastic capabilities for advanced forming applications.

2 Materials and Methods

The material used in this study was a commercial AA6061 aluminum alloy in the annealed condition. Its nominal chemical composition, in accordance with standard specifications expressed in weight percent is depicted in Tab. 1.

Cylindrical specimens were prepared with an initial diameter of 15 mm and a length of 80 mm. Prior to deformation, the specimen surfaces were polished to remove oxide layers and ensure uniform contact during processing.

The grain refinement of the AA6061 alloy was achieved using the CEE method. CEE combines both upsetting and extrusion processes, wherein the workpiece is placed in a die comprising upper and lower chambers connected through an expansion cavity. A fixed blocking funnel restricts the position of the workpiece, ensuring controlled metal flow during deformation. In each cycle, the main punch descends to extrude the material into the expansion cavity (Fig. 1a, b), after which the metal is pressed into the lower chamber once the blocking funnel is removed (Fig. 1c, d). The die can be rotated and the procedure can be repeated multiple times (Fig. 1e, f), allowing several cycles to be applied to the same workpiece. These repeated stages impart substantial plastic strain while maintaining the overall shape of the workpiece, making CEE an effective method for producing UFG structures in bulk metals.

Tab. 1 Chemical composition of AA6061

	Chemical composition of AA6061 (except for aluminum)							
Element	Mg	Si	Cu	Fe	Mn	Cr	Zn	Ti
Weight ratio [%]	1.004	0.59	0.26	0.371	0.097	0.141	0.066	0.037
Spread [±%]	0.05	0.05	0.03	0.03	0.02	0.02	0.03	0.01

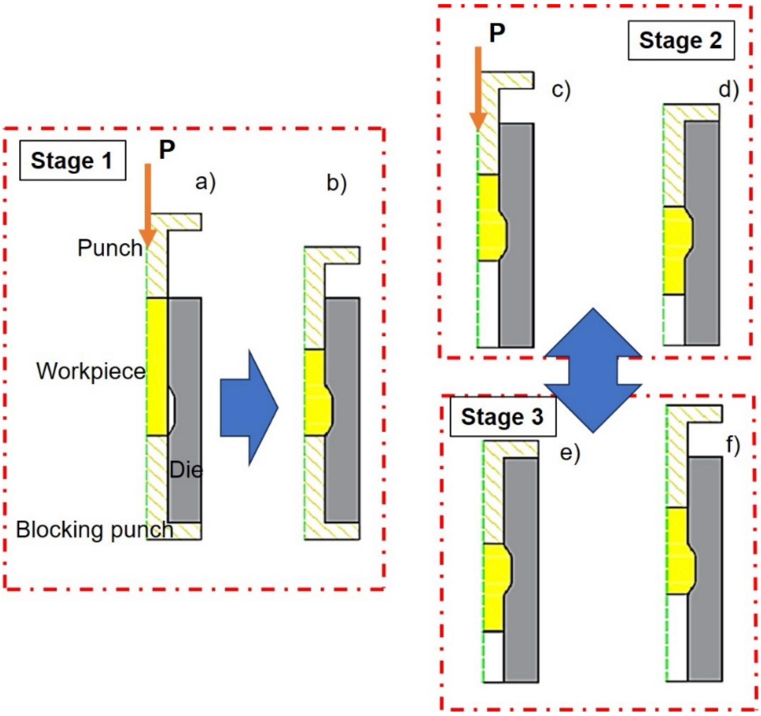

Fig. 1 Combination of upsetting and extrusion processes in one CEE cycle

Microstructural observations were carried out using an AXIO A2M optical microscope, which were performed after each cycle to evaluate the degree of grain refinement. Specimens were cut along the longitudinal axis, mechanically ground with SiC abrasive papers up to 2 000 grit, and polished with diamond suspension to obtain a reflective surface. Keller's reagent was used as the etchant to reveal grain boundaries. The average grain size was measured using the line-intercept method according to ASTM E112, based on at least five representative optical micrographs per processing condition. In this method, a set of test lines is superimposed on each micrograph, and the number of grain boundary intersections along these lines is counted to determine the mean intercept length. This value is then used to calculate the corresponding ASTM grain size number, providing a quantitative measure of the microstructure.

The mechanical response was examined by Vickers microhardness testing and uniaxial tensile testing. Microhardness measurements were performed under a load of 100 g with a dwell time of 15 s, with at least ten indentations taken at different regions of each specimen to ensure reliability. Microhardness measurements were performed using a DURAJET microhardness tester. Tensile tests were conducted on flat specimens machined from the specimens. A Devotrans DVT FU/RDNN 50 kN – CKS tensile testing machine was used for the tensile tests, featuring continuously adjustable loading speeds. Tests were carried out at 530 °C, with applied strain rates in the range of 10^{-4} to 10^{-2} s^{-1}. Elongation to failure and flow stress values were recorded to assess the superplastic response of the processed alloy.

The combination of microstructural characterization and mechanical testing provides a comprehensive basis for evaluating the relationship between grain refinement by CEE and the resulting superplastic behavior of AA6061.

3 Results and Discussion

3.1 Forming Results of the CEE Process

The CEE experiments were carried out on pre-machined AA6061 aluminum alloy specimens, following the die structure designed and optimized in the preceding simulations. The expanded section of the die has a diameter of 23 mm, which was subjected to repeated deformation cycles using the YH32–100T hydraulic press (Fig. 2a, b). Each cycle consisted of extrusion through the expansion cavity and subsequent compression, forming a continuous material flow between the upper and lower chambers of the die. After each CEE cycle, the specimens were carefully removed, cleaned, and visually examined. As shown in Fig. 2c, the deformed specimens maintained a nearly constant volume and overall geometry throughout the cycles, confirming that CEE imposes significant plastic strain without substantial material loss. However, minor forming defects such as flash formation and incomplete die filling were occasionally observed (Fig. 2d), particularly during the early cycles when frictional conditions and specimen alignment were not yet fully stabilized. These imperfections were effectively minimized through proper lubrication and adjustment of pressing parameters.

After four CEE cycles, the experimental results demonstrated that the alloy specimens could undergo repeated large plastic deformation without macroscopic cracking or delamination, highlighting the stability of the CEE die system and the suitability of AA6061 for SPD. The processed specimens exhibited uniform deformation zones, suggesting effective strain distribution within the specimen. The geometrical consistency between cycles also indicates the feasibility of using the same die configuration for multiple passes without significant wear. The successful completion of four consecutive cycles under laboratory conditions provides a solid experimental basis for further investigation of the microstructural evolution, microhardness improvement, and superplastic response of the CEE-processed AA6061 alloy.

3.2 Microstructure and Microhardness Evaluation

The evaluation of the microstructure of AA6061 alloy subjected to CEE provides fundamental insight into the mechanisms by which this SPD process enhances both strength and superplastic potential. In the annealed condition, the alloy exhibits a coarse-grained microstructure with an average grain size of approximately 100 μm.

 DOI 10.3849/aimt.02075

Such a grain morphology is typical for heat-treated AA6061 and is associated with limited ductility under conventional forming conditions. The microstructure of the AA6061 alloy after four consecutive CEE cycles was examined along both the horizontal and vertical directions of the cylindrical specimen.

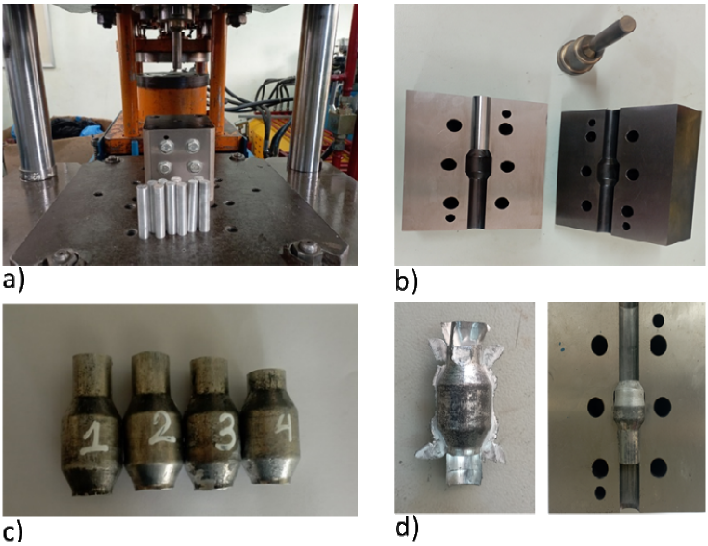

Fig. 2 Specimen and forming equipment (a); the CEE die (b); the product after CEE cycles (c); the perfective products (d)

In Fig. 3, microstructure of specimen after 1 CEE cycle is demonstrated. Despite considerable efforts using different etchants, the grain boundaries in the microstructural images can only be revealed to extent shown in Fig. 3. The metallographic samples were taken from the barrel-bulged region of the specimen in both the longitudinal and transverse directions. This location experiences the highest level of deformation; therefore, the grain refinement is expected to be the most significant there.

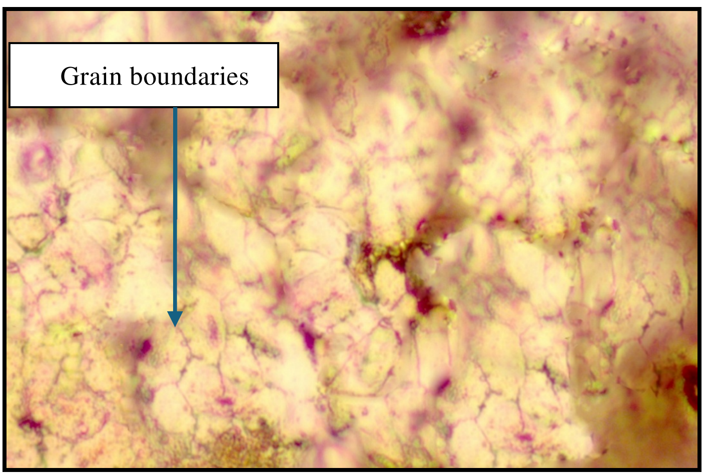

Fig. 3 Illustrative sample of microstructure in horizontal direction of specimen after 1 CEE cycle

The grain size was evaluated from optical micrographs using ImageJ software. Metallographic samples were etched with Keller's reagent and observed under an optical microscope at a magnification of 200. The scale of each image was calibrated prior to measurement, and individual grains were measured in several representative regions of the micrograph. The average grain size was calculated from the measured grain dimensions for each deformation cycle. Grain sizes of specimen in horizontal and vertical directions for 1 to 4 CEE cycles are shown in Fig. 4.

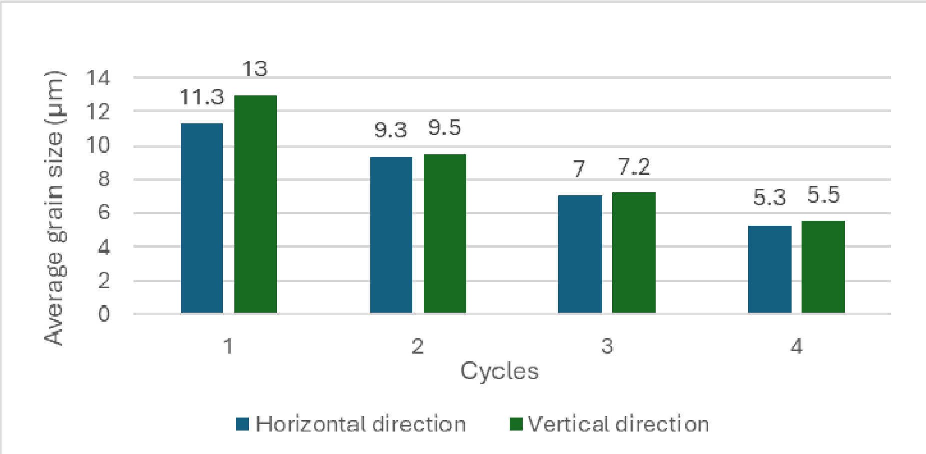

Fig. 4 Grain sizes of specimen after 1 *to* 4 *CEE cycles along the horizontal and vertical direction*

After the first cycle of CEE, significant fragmentation of coarse grains is observed, with the average grain size reduced to around (11–13) µm. This rapid reduction indicates that CEE imposes intense plastic strain during the initial passes, accelerating the subdivision of grains through mechanisms of dislocation accumulation and formation of subgrain boundaries.

With successive CEE cycles, continued grain refinement occurs as the dislocation structures evolve into more stable, equiaxed subgrains. After two cycles, the grain size is refined further to approximately (9–10) µm, approaching the threshold typically required for the onset of superplasticity in aluminum alloys. Beyond this point, the refinement rate slows slightly, as the microstructure transitions from a heavily strained, heterogeneous state to a more stable UFG configuration. By the fourth CEE cycle, the microstructure stabilizes at an average grain size of about (5–6) µm, demonstrating the effectiveness of CEE in generating UFG structures without the need for elevated-temperature processing. The resulting grains are equiaxed and uniformly distributed, which is crucial for ensuring homogeneous deformation during subsequent high-temperature testing.

This progressive grain refinement can be attributed to continuous dynamic recrystallization (CDRX) [24, 25]. In CEE, the alternating compression and extrusion steps generate high dislocation densities that rearrange into low-angle boundaries. As strain accumulates, these boundaries gradually evolve into high-angle grain boundaries, completing the transformation into new fine grains. Unlike static recrystallization, which requires thermal activation, CDRX occurs in situ during deformation, allowing refinement even at room temperature. This mechanism explains the substantial microstructural stability observed in AA6061 after multiple CEE cycles.

The microhardness evolution of AA6061 aluminum alloy was systematically investigated following successive CEE processing. The initial material exhibited a relatively coarse-grained microstructure with a Vickers microhardness of approximately 40 HV. This baseline characterization confirmed that the alloy possessed high strength, specific strength, and good wear resistance prior to severe plastic deformation. The microhardness of the deformed specimens was measured along both the horizontal and vertical directions on their longitudinal cross-sections for specimens subjected to 1, 2, 3, and 4 CEE cycles. The measurement locations and procedure were carefully controlled to ensure consistency and reliability, allowing accurate comparison of microhardness variations across different cycles. The layout of the examined localities is shown in Fig. 5.

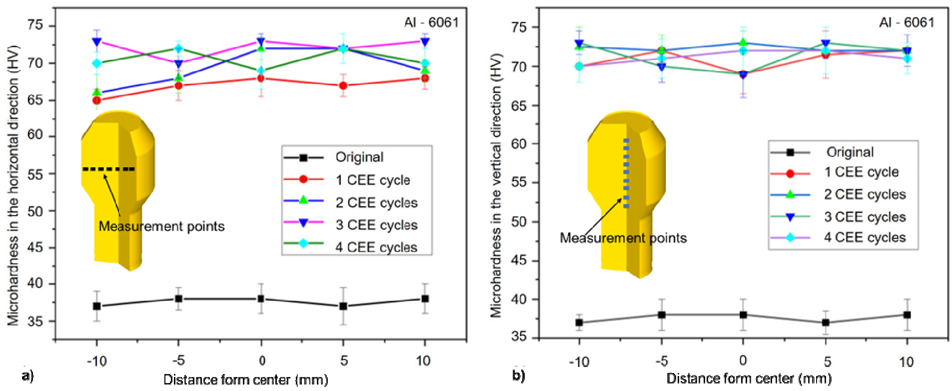

Fig. 5 Microhardness measured along the horizontal (a) and vertical (b) directions relative to the specimen axis, for the original material and after 1 *to* 4 *CEE cycles.*

The evolution of microhardness in AA6061 aluminum alloy subjected to CEE was systematically investigated, revealing a clear relationship between accumulated plastic strain and mechanical response. As shown in Fig. 5, the average microhardness of the specimens increased sharply after the first CEE cycle, rising from 40 HV to approximately 65 HV, indicating pronounced work hardening due to the initial plastic deformation. Following the second cycle, only a minor increase in microhardness was observed, while in subsequent cycles (third and fourth), the values stabilized around 70 HV. This trend is consistent with microstructural evolution, where significant grain refinement occurs during the first cycles, but the rate of refinement decreases as the structure approaches a UFG configuration. The limited change in microhardness in later cycles reflects the saturation of accumulated strain and the transition from work-hardening-dominated behavior to a more stable, fine-grained microstructure with enhanced ductility. These findings highlight a key characteristic of SPD techniques: the ability to rapidly increase hardness through initial deformation, followed by stabilization as the material structure equilibrates. Overall, the results demonstrate the effectiveness of CEE in improving the mechanical properties of AA6061 through controlled grain refinement, providing a balance between strength and ductility suitable for UFG aluminum alloys.

3.3 Superplastic Deformation Behavior of AA6061 Alloy after CEE

The UFG structure generated in AA6061 through cyclic expansion–extrusion (CEE) provides favorable conditions for superplastic deformation. The refined microstructure achieved after four CEE cycles, with an average grain size of (5–6) μm, satisfies these microstructural requirements and enables grain boundary–controlled mechanisms to dominate during high-temperature deformation. The cylindrical specimens after 3 and 4 CEE cycles (CEE-3 and CEE-4) were subjected to superplastic tensile tests at a temperature of 530 °C with different strain rates of 10^{-4}, 10^{-3}, and 10^{-2} s^{-1}.

This observation also explains the trend in which relative elongation increases as the average grain size decreases in CEE-processed specimens. As shown in Tab. 2, the tensile response of AA6061 alloy subjected to 3 and 4 cycles of CEE demonstrates a clear distinction. When tested at the same temperatures and strain rates, specimens processed through four CEE cycles (CEE-4) consistently exhibit higher relative elongation than those processed through three cycles (CEE-3). Specifically, the increase in elongation reaches ~30 %, 65 %, and 25 % at strain rates of 10^{-4} s^{-1}, 10^{-3} s^{-1}, and 10^{-2} s^{-1}, respectively. These improvements are closely linked to the reduced grain size achieved in the CEE-processed specimens. From a mechanistic perspective, GBS remains the dominant mechanism controlling superplastic deformation. GBS accommodates large strains while maintaining equiaxed grain structures, enabling grain rotation and texture evolution. Evidence of GBS is observed as relative displacement between adjacent grains along their boundaries, ultimately leading to the replacement of neighboring grains, a characteristic phenomenon of superplasticity absent in conventional plastic deformation [26, 27]. Under superplastic conditions, individual grains undergo minimal morphological changes. Even if some grains appear slightly elongated, their deformation is much smaller than the overall elongation of the specimen. The near-constant grain shape within the superplastic strain rate regime indicates that the majority of deformation arises from relative displacement between neighboring grains, enhancing grain density along the tensile direction and resulting in high elongation. According to the GBS mechanism, deformation is concentrated at grain boundaries. Therefore, reducing grain size increases total grain boundary area, facilitating higher relative elongation under tensile loading.

Tab. 2 Tensile test results of the CEE-processed specimens at different strain rates

Specimens	Elongations [%]		
	Strain rate 10^{-4} s^{-1}	Strain rate 10^{-3} s^{-1}	Strain rate 10^{-2} s^{-1}
CEE-3	180	200	160
CEE-4	230	330	200

The presence of ultrafine grains in CEE-processed specimens confirms the manifestation of superplasticity in AA6061 alloy, as verified by tensile tests under superplastic conditions. All specimens displayed elongations exceeding 150 % with relatively low flow stresses. Comparative analysis of tensile behavior of specimens from CEE-3 and CEE-4 (Tab. 2) reveals a strong dependence on strain rate. As the strain rate increases from 10^{-4} s^{-1} to 10^{-3} s^{-1}, relative elongation improves, while further increase to 10^{-2} s^{-1} leads to a decrease in elongation. For CEE-4 specimens, the maximum elongations at strain rates of 10^{-4} s^{-1}, 10^{-3} s^{-1}, and 10^{-2} s^{-1} were 230 %, 330 %, and 200 %, respectively (Fig. 6a). In contrast, CEE-3 specimens exhibited elongations of 100 %, 200 %, and 160 % at corresponding strain rates (Fig. 6b). These results highlight the strong influence of strain rate on the superplastic response of UFG AA6061 processed by CEE. At strain rates below 10^{-4} s^{-1}, excessive grain growth due to CDRX induces premature necking, limiting elongation [26, 27]. Conversely, at strain rates above10^{-2} s^{-1}, deformation occurs faster than diffusion-assisted mechanisms can accommodate favorable sliding, leading to higher flow stress and reduced ductility [28, 29]. The optimal superplastic response was observed at a strain rate of 10^{-3} s^{-1}, achieving maximum elongations of 200 % for CEE-3 and 330 % for CEE-4 specimens.

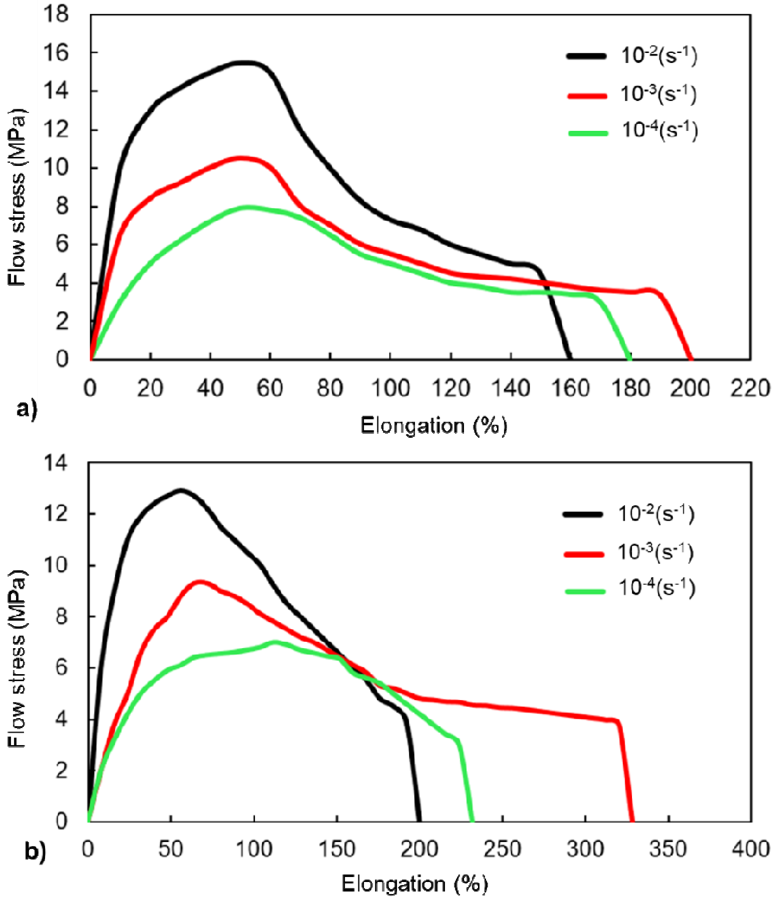

Fig. 6 The flow stress – relative elongation curves at 530 °C *for the* CEE-3 *specimens (a), the* CEE-4 *specimens (b) with different strain rates*

Fig. 6 also illustrates the combined effect of grain size and superplastic strain rate on maximum flow stress. CEE-4 specimens, with finer grains, consistently display lower flow stress than CEE-3 specimens across all tested strain rates. Specifically, flow stresses for CEE-4 specimens at 10^{-4} s^{-1}, 10^{-3} s^{-1}, and 10^{-2} s^{-1} are 7 MPa, 9.5 MPa, and 13 MPa, compared to 8 MPa, 10.5 MPa, and 15.5 MPa for CEE-3 specimens. These differences are attributed to the initial UFG microstructure in CEE-4, which increases grain boundary area, promoting GBS and more uniform plastic flow, thereby reducing flow stress. Additionally, an increasing trend of flow stress with strain rate is observed: at low strain rates and high temperatures, sufficient atomic diffusion facilitates favorable slip planes, reducing flow resistance, whereas at higher strain rates, limited diffusion leads to increased flow stress.

4 Conclusions

In this study, the superplastic properties of UFG AA6061 aluminum alloy processed by CEE were investigated. Based on the experimental results and comparative analysis, the following conclusions can be drawn:

- The CEE process successfully reduced the average grain size of AA6061 to ~5-6 μm after four cycles, providing the essential structural condition for superplasticity. The refined and stable grain structure promotes GBS and supports CDRX during high-temperature deformation.
- The microhardness of AA6061 increased from about 40 HV to ~70 HV after four CEE cycles, indicating a 75 % enhancement. This improvement results from intense strain hardening and grain refinement, leading to a stable UFG structure with improved strength.
- Specimens subjected to three and four cycles of CEE exhibited evident superplastic characteristics when tested at 530 °C under various strain rates (10^{-4} s^{-1}, 10^{-3} s^{-1}, and 10^{-2} s^{-1}). All specimens showed elongations beyond 150 % with relatively low flow stresses. The most favorable superplastic response was obtained in the CEE-4 specimen at a strain rate of 10^{-3} s^{-1}, achieving a maximum elongation of 330 % accompanied by a low flow stress of about 9.5 MPa.
- The results confirm that CEE not only enhances the mechanical strength of AA6061 at room temperature but also provides a stable UFG microstructure suitable for SPF. This makes CEE-processed AA6061 a promising candidate for lightweight structural components requiring complex geometries and superior ductility.

The superplastic forming capability of AA6061 aluminum alloy enables the production of lightweight structural components with complex geometries, making it suitable for applications such as UAV airframe parts, sensor housings, and protective covers in military systems. This approach allows for a reduction in the number of joints and overall structural weight while maintaining adequate mechanical performance.

Acknowledgement

The authors acknowledge the support of Le Quy Don Technical University, Hanoi, Vietnam, and thank colleagues and technicians for their assistance with experiments and data analysis. This publication was partly created in cooperation with the University of Defence in Brno based on specific research project SV24-201.

References

[1] SUN, Y. The Use of Aluminum Alloys in Structures: Review and Outlook. *Structures*, 2023, **57**, 105290. DOI 10.1016/j.istruc.2023.105290.

[2] KHALAFE, W.H., E.L. SHENG, M.R.B. ISA and S.B. SHAMSUDIN. Enhancing Mechanical Characteristics of 6061-T6 with 5083-H111 Aluminium Alloy Dissimilar Weldments: A New Pin Tool Design for Friction Stir Welding (FSW). *Metals*, 2024, **14**(5), 534. DOI 10.3390/met14050534.

[3] LUO, Z., X. ZHANG, Z. LIU, H. ZHOU, M. WANG and G. XIE. Mechanical Properties and Interfacial Characteristics of 6061 Al Alloy Plates Fabricated by Hot-Roll Bonding. *International Journal of Minerals, Metallurgy and Materials*, 2024, **31**, pp. 1890-1899. DOI 10.1007/s12613-023-2801-8.

[4] HUANG, Y. and T.G. LANGDON. Advances in Ultrafine-Grained Materials. *Materials Today*, 2013, **16**(3), pp. 85-93. DOI 10.1016/j.mattod.2013.03.004.

[5] EDALATI, K., et al. Nanomaterials by Severe Plastic Deformation: Review of Historical Developments and Recent Advances. *Materials Research Letters*, 2022, **10**(4), pp. 163-256. DOI 10.1080/21663831.2022.2029779.

[6] NGUYEN, Q.C., D. OLASZ, A.Q. AHMED, E.V. BOBRUK and R.Z. VALIEV. Review on Grain Size- and Grain Boundary Phenomenon in Unusual Mechanical Behavior of Ultrafine-Grained Al Alloys. *Materials Transactions*, 2023, **64**(8), pp. 1844-1855. DOI 10.2320/matertrans.MT-MF2022020.

[7] LAPLANCHE, G., T. HIGASHI and M.J. STARINK. Grain Boundary Sliding and Strain Rate Sensitivity of Coarse and Fine/Ultrafine Grained 5083 Aluminum Alloys. *Metallurgical and Materials Transactions A*, 2020, **51**(1), pp. 1109-1122. DOI 10.1007/s11661-019-05583-5.

[8] KWEITSU, E.K., D.K. SARKAR and X.-G. CHEN. A Short Review on Superplasticity of Aluminum Alloys. *Engineering Proceedings*, 2023, **43**(1), 43. DOI 10.3390/engproc2023043043.

[9] BHATTA, L., A. PESIN, A.P. ZHILYAEV, P. TANDON, C. KONG and H. YU. Recent Development of Superplasticity in Aluminum Alloys: A Review. *Metals*, 2020, **10**(1), 77. DOI 10.3390/met10010077.

[10] BOBRUK, E.V., N.G. ZARIPOV, I.A. RAMAZANOV, N.Q. CHINH and R.Z. VALIEV. Low-Temperature Superplasticity of Ultrafine-Grained Aluminum Alloys: Recent Discoveries and Innovative Potential. *Materials*, 2024, **17**(13), 3311. DOI 10.3390/ma17133311.

[11] ZRNÍK, J., S.V. DOBATKIN and I. MAMUZI. Processing of Metals by Severe Plastic Deformation (SPD) – Structure and Mechanical Properties Respond. *Metalurgija*, 2008, **47**(3), pp. 211-216. ISSN 0543-5846.

[12] VALIEV, R.Z., R.K. ISLAMGALIEV and I.V. ALEXANDROV. Bulk Nanostructured Materials from Severe Plastic Deformation. *Progress in Materials Science*, 2000, **45**(2), pp. 103-189. DOI 10.1016/S0079-6425(99)00007-9.

[13] LI, X., M. DU, Z. MAO, T. HUANG and C. BAN. Recent Advances in the Equal Channel Angular Pressing of Metallic Materials. *Processes*, 2022, **10**(11), 2181. DOI 10.3390/pr10112181.

[14] ZHILYAEV, A.P. and T.G. LANGDON. Using High-Pressure Torsion for Metal Processing: Fundamentals and Applications. *Progress in Materials Science*, 2008, **53**(6), pp. 893-979. DOI 10.1016/j.pmatsci.2008.03.002.

[15] NGUYEN, M.T., V.T. LE, M.H. LE and T.A. NGUYEN. Superplastic Properties in a Ti5Al3Mo1.5V Titanium Alloy Processed by Multidirectional Forging Process. *Materials Letters*, 2022, **307**, 131004. DOI 10.1016/j.matlet.2021.131004.

[16] RICHERT, M., H. PETRYK and S. STUPKIEWICZ. Grain Refinement in AlMg-Si Alloy during Cyclic Extrusion–Compression: Experiment and Modelling. *Archives of Metallurgy and Materials*, 2007, **52**(1), pp. 49-54. ISSN 1733-3490.

[17] PARDIS, N., B. TALEBANPOUR, R. EBRAHIMI and Z. ZOMORODIAN. Cyclic Expansion–Extrusion (CEE): A Modified Counterpart of Cyclic Extrusion–Compression (CEC). *Materials Science and Engineering A*, 2011, **528**, pp. 7537-7540. DOI 10.1016/j.msea.2011.06.059.

[18] KRATOCHVÍL, J. Mechanism of Grain Refinement Induced by Severe Plastic Deformation. *Materials Science Forum*, 2010, **667-669**, pp. 617-622. DOI 10.4028/www.scientific.net/MSF.667-669.617.

[19] TRUONG, D.X., M.T. NGUYEN, M.H. NGUYEN and T.A. NGUYEN. Effect of the Cyclic Expansion–Extrusion Process on Mechanical Properties and the Grain Refinement of AA6061 Aluminum Alloy. *Journal of Military Science and Technology*, 2023, **87**, pp. 100-107. DOI 10.54939/1859-1043.j.mst.87.2023.100-107.

[20] NGUYEN, M.T. Experimental Determination of Process Parameters for Superplastic Forming from AA7075 Aluminum Alloy [online]. *Suranaree Journal of Science and Technology*, 2022, **29**(5), 010163(1-6) [viewed 2025-11-09]. Available from: https://ird.sut.ac.th/e-journal/Journal/pdf/220104793.pdf

[21] KAIBYSHEV, R., F. MUSIN and D.R. LESUER. Superplasticity in Al–Mg–Sc–Zr Alloys Processed by Equal-Channel Angular Pressing. *Acta Materialia*, 2005, **53**(15), pp. 4053-4064. DOI 10.1016/j.actamat.2005.05.020.

[22] XU, C., Z. HORITA and T.G. LANGDON. Superplasticity in an Al–Cu Alloy Processed by Equal-Channel Angular Pressing. *Acta Materialia*, 2008, **56**(6), pp. 1435-1446. DOI 10.1016/j.actamat.2007.12.007.

[23] NGUYEN, M.T. and T.A. NGUYEN. Microstructure and Microhardness of AA6061 Aluminum Alloy Formed by Cyclic Expansion–Extrusion Process: Numerical Simulation and Experimental Evaluation. *Archives of Metallurgy and Materials*, 2025, **70**(2), pp. 625-632. DOI 10.24425/amm.2025.153463.

[24] BACCA, M., D.R. HAYHURST and R.M. MCMEEKING. Continuous Dynamic Recrystallization during Severe Plastic Deformation. *Mechanics of Materials*, 2015, **90**, pp. 148-156. DOI 10.1016/j.mechmat.2015.05.008.

[25] YANG, Q., T. WOJCIK and E. KOZESCHNIK. Continuous Dynamic Recrystallization and Deformation Behavior of an AA1050 Aluminum Alloy during High-Temperature Compression. *Metals*, 2024, **14**(8), 889. DOI 10.3390/met14080889.

[26] KAIBYSHEV, R., A. GOLOBORODKO, F. MUSIN, I. NIKULIN and T. SAKAI. The Role of Grain Boundary Sliding in Microstructural Evolution during Superplastic Deformation of a 7055 Aluminum Alloy. *Materials Transactions*, 2002, **43**(10), pp. 2408-2414. DOI 10.2320/matertrans.43.2408.

[27] KUZNETSOV, A., L. KARKINA, Y. GORNOSTYREV and P. KORZHAVYI. Effects of Zn and Mg Segregations on the Grain Boundary Sliding and Cohesion in Al: Ab Initio Modelling. *Metals*, 2021, **11**(4), 631. DOI 10.3390/met11040631.

[28] YAKOVTSEVA, O., M. SITKINA, A.O. MOSLEH and A. MIKHAYLOVSKAYA. High Strain Rate Superplasticity in Al–Zn–Mg-Based Alloy: Microstructural Design, Deformation Behavior, and Modeling. *Materials*, 2020, **13**(9), 2098. DOI 10.3390/ma13092098.

[29] LEE, S., K. WATANABE, K. MATSUDA and Z. HORITA. Low-Temperature and High-Strain-Rate Superplasticity of Ultrafine-Grained A7075 Processed by High-Pressure Torsion. *Materials Transactions*, 2018, **59**(8), pp. 1341-1347. DOI 10.2320/matertrans.L-M2018825.